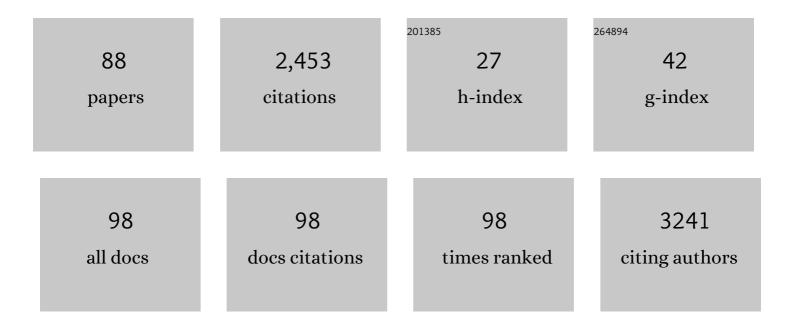
Yen-Yu Ian Shih

List of Publications by Year in descending order

Source: https://exaly.com/author-pdf/731950/publications.pdf Version: 2024-02-01



ΥΕΝ-ΥΠΙΛΝ ΟΗΙΗ

| # | Article | IF | CITATIONS |
|----|--|-----|-----------|
| 1 | Computing hemodynamic response functions from concurrent spectral fiber-photometry and fMRI data. Neurophotonics, 2022, 9, 032205. | 1.7 | 13 |
| 2 | Chemogenetic stimulation of tonic locus coeruleus activity strengthens the default mode network. Science Advances, 2022, 8, eabm9898. | 4.7 | 36 |
| 3 | Spectral fiber photometry derives hemoglobin concentration changes for accurate measurement of fluorescent sensor activity. Cell Reports Methods, 2022, 2, 100243. | 1.4 | 23 |
| 4 | Superoxide free radical spinâ€lattice relaxivity: A quenchâ€assisted MR study. Magnetic Resonance in Medicine, 2021, 86, 1058-1066. | 1.9 | 2 |
| 5 | Vibration-Assisted Insertion of Flexible Neural Microelectrodes With Bio-Dissolvable Guides for Medical Implantation. , 2021, , . | | 1 |
| 6 | One-pot synthesis of carboxymethyl-dextran coated iron oxide nanoparticles (CION) for preclinical fMRI and MRA applications. NeuroImage, 2021, 238, 118213. | 2.1 | 19 |
| 7 | An isotropic EPI database and analytical pipelines for rat brain resting-state fMRI. NeuroImage, 2021, 243, 118541. | 2.1 | 20 |
| 8 | Simultaneous fMRI and fast-scan cyclic voltammetry bridges evoked oxygen and neurotransmitter dynamics across spatiotemporal scales. NeuroImage, 2021, 244, 118634. | 2.1 | 10 |
| 9 | Altered Cortico-Subcortical Network After Adolescent Alcohol Exposure Mediates Behavioral Deficits in Flexible Decision-Making. Frontiers in Pharmacology, 2021, 12, 778884. | 1.6 | 4 |
| 10 | 3D U-Net Improves Automatic Brain Extraction for Isotropic Rat Brain Magnetic Resonance Imaging Data. Frontiers in Neuroscience, 2021, 15, 801008. | 1.4 | 9 |
| 11 | The Accumulation of Tau-Immunoreactive Hippocampal Granules and Corpora Amylacea Implicates Reactive Glia in Tau Pathogenesis during Aging. IScience, 2020, 23, 101255. | 1.9 | 17 |
| 12 | Automatic Skull Stripping of Rat and Mouse Brain MRI Data Using U-Net. Frontiers in Neuroscience, 2020, 14, 568614. | 1.4 | 38 |
| 13 | Mitochondriotropic lanthanide nanorods: implications for multimodal imaging. Chemical Communications, 2020, 56, 7945-7948. | 2.2 | 12 |
| 14 | Supramammillary nucleus synchronizes with dentate gyrus to regulate spatial memory retrieval through glutamate release. ELife, 2020, 9, . | 2.8 | 30 |
| 15 | Loss of Brain Norepinephrine Elicits Neuroinflammation-Mediated Oxidative Injury and Selective Caudo-Rostral Neurodegeneration. Molecular Neurobiology, 2019, 56, 2653-2669. | 1.9 | 50 |
| 16 | MR imaging central thalamic deep brain stimulation restored autistic-like social deficits in the rat. Brain Stimulation, 2019, 12, 1410-1420. | 0.7 | 15 |
| 17 | Noradrenergic dysfunction accelerates LPS-elicited inflammation-related ascending sequential neurodegeneration and deficits in non-motor/motor functions. Brain, Behavior, and Immunity, 2019, 81, 374-387. | 2.0 | 36 |
| 18 | A subset of noradrenergic (NE) neurons defined by developmental expression of Hoxb1 have a distinct role in attenuating the behavioral response to acute stress. Molecular Psychiatry, 2019, 24, 625-625. | 4.1 | 0 |

Yen-Yu Ian Shih

| # | Article | IF | CITATIONS |
|----|--|-----|-----------|
| 19 | Genetic identification of a population of noradrenergic neurons implicated in attenuation of stress-related responses. Molecular Psychiatry, 2019, 24, 710-725. | 4.1 | 24 |
| 20 | Animal Functional Magnetic Resonance Imaging: Trends and Path Toward Standardization. Frontiers in Neuroinformatics, 2019, 13, 78. | 1.3 | 78 |
| 21 | An Adeno-Associated Virus-Based Toolkit for Preferential Targeting and Manipulating Quiescent Neural Stem Cells in the Adult Hippocampus. Stem Cell Reports, 2018, 10, 1146-1159. | 2.3 | 12 |
| 22 | Simultaneous functional photoacoustic microscopy and electrocorticography reveal the impact of rtPA on dynamic neurovascular functions after cerebral ischemia. Journal of Cerebral Blood Flow and Metabolism, 2018, 38, 980-995. | 2.4 | 15 |
| 23 | Adolescent alcohol exposure decreases frontostriatal restingâ€state functional connectivity in adulthood. Addiction Biology, 2018, 23, 810-823. | 1.4 | 58 |
| 24 | IL-11 antagonist suppresses Th17 cell-mediated neuroinflammation and demyelination in a mouse model of relapsing-remitting multiple sclerosis. Clinical Immunology, 2018, 197, 45-53. | 1.4 | 12 |
| 25 | Role of Genetic Variation in Collateral Circulation in the Evolution of Acute Stroke. Stroke, 2017, 48, 754-761. | 1.0 | 24 |
| 26 | Functional circuit mapping of striatal output nuclei using simultaneous deep brain stimulation and fMRI. NeuroImage, 2017, 146, 1050-1061. | 2.1 | 32 |
| 27 | Coordination of Brain-Wide Activity Dynamics by Dopaminergic Neurons. Neuropsychopharmacology, 2017, 42, 615-627. | 2.8 | 59 |
| 28 | Structural and functional connectivity between the lateral posterior–pulvinar complex and primary visual cortex in the ferret. European Journal of Neuroscience, 2016, 43, 230-244. | 1.2 | 15 |
| 29 | Functional Magnetic Resonance Imaging of Electrical and Optogenetic Deep Brain Stimulation at the Rat Nucleus Accumbens. Scientific Reports, 2016, 6, 31613. | 1.6 | 32 |
| 30 | Resting state network topology of the ferret brain. NeuroImage, 2016, 143, 70-81. | 2.1 | 30 |
| 31 | Combining optogenetic stimulation and fMRI to validate a multivariate dynamical systems model for estimating causal brain interactions. NeuroImage, 2016, 132, 398-405. | 2.1 | 60 |
| 32 | Aging and Microglial Activation in Neurodegenerative Diseases. Oxidative Stress in Applied Basic Research and Clinical Practice, 2016, , 107-131. | 0.4 | 0 |
| 33 | Robust deep brain stimulation functional MRI procedures in rats and mice using an MR-compatible tungsten microwire electrode. Magnetic Resonance in Medicine, 2015, 73, 1246-1251. | 1.9 | 29 |
| 34 | Temporal assessment of vascular reactivity and functionality using MRI during postischemic proangiogenenic vascular remodeling. Magnetic Resonance Imaging, 2015, 33, 903-910. | 1.0 | 2 |
| 35 | Rescue of cortical neurovascular functions during the hyperacute phase of ischemia by peripheral sensory stimulation. Neurobiology of Disease, 2015, 75, 53-63. | 2.1 | 33 |
| 36 | Assessment of neurovascular dynamics during transient ischemic attack by the novel integration of micro-electrocorticography electrode array with functional photoacoustic microscopy. Neurobiology of Disease, 2015, 82, 455-465. | 2.1 | 26 |

YEN-YU IAN SHIH

| # | Article | IF | CITATIONS |
|----|---|-----|-----------|
| 37 | Aspm sustains postnatal cerebellar neurogenesis and medulloblastoma growth. Development (Cambridge), 2015, 142, 3921-32. | 1.2 | 54 |
| 38 | Advances in Molecular Pathway-Directed Cancer Systems Imaging and Therapy. BioMed Research International, 2014, 2014, 1-2. | 0.9 | 4 |
| 39 | Comparison of retinal and cerebral blood flow between continuous arterial spin labeling MRI and fluorescent microsphere techniques. Journal of Magnetic Resonance Imaging, 2014, 40, 609-615. | 1.9 | 13 |
| 40 | Functional MRI reveals frequency-dependent responses during deep brain stimulation at the subthalamic nucleus or internal globus pallidus. NeuroImage, 2014, 84, 11-18. | 2.1 | 62 |
| 41 | Dynamic perfusion and diffusion MRI of cortical spreading depolarization in photothrombotic ischemia. Neurobiology of Disease, 2014, 71, 131-139. | 2.1 | 29 |
| 42 | Imaging Neurovascular Function and Functional Recovery after Stroke in the Rat Striatum Using Forepaw Stimulation. Journal of Cerebral Blood Flow and Metabolism, 2014, 34, 1483-1492. | 2.4 | 34 |
| 43 | fMRI of Deep Brain Stimulation at the Rat Ventral Posteromedial Thalamus. Brain Stimulation, 2014, 7, 190-193. | 0.7 | 21 |
| 44 | Deep Brain Stimulation with Simultaneous fMRI in Rodents. Journal of Visualized Experiments, 2014, , e51271. | 0.2 | 16 |
| 45 | MRI study of cerebral, retinal and choroidal blood flow responses to acute hypertension. Experimental Eye Research, 2013, 112, 118-124. | 1.2 | 19 |
| 46 | Ultra high-resolution fMRI and electrophysiology of the rat primary somatosensory cortex. NeuroImage, 2013, 73, 113-120. | 2.1 | 44 |
| 47 | Dopaminergic imaging of nonmotor manifestations in a rat model of Parkinson's disease by fMRI. Neurobiology of Disease, 2013, 49, 99-106. | 2.1 | 22 |
| 48 | Methylene blue potentiates stimulus-evoked fMRI responses and cerebral oxygen consumption during normoxia and hypoxia. NeuroImage, 2013, 72, 237-242. | 2.1 | 38 |
| 49 | Quantitative Retinal and Choroidal Blood Flow During Light, Dark Adaptation and Flicker Light Stimulation in Rats Using Fluorescent Microspheres. Current Eye Research, 2013, 38, 292-298. | 0.7 | 42 |
| 50 | Chronic Rapamycin Restores Brain Vascular Integrity and Function Through NO Synthase Activation and Improves Memory in Symptomatic Mice Modeling Alzheimer's Disease. Journal of Cerebral Blood Flow and Metabolism, 2013, 33, 1412-1421. | 2.4 | 181 |
| 51 | Neural Circuit Modulation During Deep Brain Stimulation at the Subthalamic Nucleus for Parkinson's Disease: What Have We Learned from Neuroimaging Studies?. Brain Connectivity, 2013, 4, 131218075844008. | 0.8 | 18 |
| 52 | High-Resolution 3D MR Microangiography of the Rat Ocular Circulation. Radiology, 2012, 264, 234-241. | 3.6 | 21 |
| 53 | Investigation of the cerebral hemodynamic response function in single blood vessels by functional photoacoustic microscopy. Journal of Biomedical Optics, 2012, 17, 061210. | 1.4 | 30 |
| 54 | Transcranial Imaging of Functional Cerebral Hemodynamic Changes in Single Blood Vessels using <i>in vivo</i> Photoacoustic Microscopy. Journal of Cerebral Blood Flow and Metabolism, 2012, 32, 938-951. | 2.4 | 77 |

Yen-Yu Ian Shih

| # | Article | IF | CITATIONS |
|----|--|-----|-----------|
| 55 | Layer-specific blood-flow MRI of retinitis pigmentosa in RCS rats. Experimental Eye Research, 2012, 101, 90-96. | 1.2 | 31 |
| 56 | Design, simulation and experimental validation of a novel flexible neural probe for deep brain stimulation and multichannel recording. Journal of Neural Engineering, 2012, 9, 036001. | 1.8 | 72 |
| 57 | 3D magnetic resonance microscopy of the ex vivo retina. Magnetic Resonance in Medicine, 2012, 67, 1154-1158. | 1.9 | 4 |
| 58 | Pharmacological MRI of the choroid and retina: Blood flow and BOLD responses during nitroprusside infusion. Magnetic Resonance in Medicine, 2012, 68, 1273-1278. | 1.9 | 24 |
| 59 | Layer-Specific Manganese-Enhanced MRI of the Retina in Light and Dark Adaptation. , 2012, 53, 4352. | | 13 |
| 60 | Correction of inhomogeneous magnetic resonance images using multiscale retinex for segmentation accuracy improvement. Biomedical Signal Processing and Control, 2012, 7, 129-140. | 3.5 | 7 |
| 61 | Endogenous opioid–dopamine neurotransmission underlie negative CBV fMRI signals. Experimental Neurology, 2012, 234, 382-388. | 2.0 | 26 |
| 62 | A low cost color visual stimulator for fMRI. Journal of Neuroscience Methods, 2012, 204, 379-382. | 1.3 | 5 |
| 63 | A rare case of coiling of the brachial artery: a description of the sonographic features. Journal of Medical Ultrasonics (2001), 2012, 39, 21-24. | 0.6 | 1 |
| 64 | Striatal and Cortical BOLD, Blood Flow, Blood Volume, Oxygen Consumption, and Glucose Consumption Changes in Noxious Forepaw Electrical Stimulation. Journal of Cerebral Blood Flow and Metabolism, 2011, 31, 832-841. | 2.4 | 60 |
| 65 | Blood oxygenation levelâ€dependent (BOLD) functional MRI of visual stimulation in the rat retina at 11.7 T. NMR in Biomedicine, 2011, 24, 188-193. | 1.6 | 23 |
| 66 | Longitudinal study of tumorâ€associated macrophages during tumor expansion using MRI. NMR in Biomedicine, 2011, 24, 1353-1360. | 1.6 | 28 |
| 67 | Automatic spike sorting for extracellular electrophysiological recording using unsupervised single linkage clustering based on grey relational analysis. Journal of Neural Engineering, 2011, 8, 036003. | 1.8 | 14 |
| 68 | Lamina-Specific Functional MRI of Retinal and Choroidal Responses to Visual Stimuli. , 2011, 52, 5303. | | 32 |
| 69 | Subcutaneous lipoma compressing the common peroneal nerve and causing palsy: Sonographic diagnosis. Journal of Clinical Ultrasound, 2010, 38, 97-99. | 0.4 | 7 |
| 70 | Intramuscular Schwannoma Arising from the Psoas Muscle Presenting with Femoral Nerve Neuropathy. Southern Medical Journal, 2010, 103, 477-479. | 0.3 | 10 |
| 71 | Quantitative MR T2 measurement of articular cartilage to assess the treatment effect of intra-articular hyaluronic acid injection on experimental osteoarthritis induced by ACLX. Osteoarthritis and Cartilage, 2010, 18, 54-60. | 0.6 | 22 |
| 72 | MicroPET imaging of noxious thermal stimuli in the conscious rat brain. Somatosensory & Motor Research, 2010, 27, 69-81. | 0.4 | 17 |

YEN-YU IAN SHIH

| # | Article | IF | CITATIONS |
|----|--|-----|-----------|
| 73 | Superior-capsular elongation and its significance in atraumatic posteroinferior multidirectional shoulder instability in magnetic resonance arthrography. Acta Radiologica, 2010, 51, 302-308. | 0.5 | 18 |
| 74 | Imaging brain hemodynamic changes during rat forepaw electrical stimulation using functional photoacoustic microscopy. Neurolmage, 2010, 52, 562-570. | 2.1 | 111 |
| 75 | A New Scenario for Negative Functional Magnetic Resonance Imaging Signals: Endogenous Neurotransmission. Journal of Neuroscience, 2009, 29, 3036-3044. | 1.7 | 114 |
| 76 | Automatic segmentation of magnetic resonance images using a decision tree with spatial information. Computerized Medical Imaging and Graphics, 2009, 33, 111-121. | 3.5 | 18 |
| 77 | MicroPET study of brain neuronal metabolism under electrical and mechanical stimulation of the rat tail. Nuclear Medicine Communications, 2009, 30, 188-193. | 0.5 | 14 |
| 78 | Wholeâ€brain functional magnetic resonance imaging mapping of acute nociceptive responses induced by formalin in rats using atlas registrationâ€based eventâ€related analysis. Journal of Neuroscience Research, 2008, 86, 1801-1811. | 1.3 | 45 |
| 79 | BOLD fMRI mapping of brain responses to nociceptive stimuli in rats under ketamine anesthesia. Medical Engineering and Physics, 2008, 30, 953-958. | 0.8 | 26 |
| 80 | Improving segmentation accuracy for magnetic resonance imaging using a boosted decision tree. Journal of Neuroscience Methods, 2008, 175, 206-217. | 1.3 | 8 |
| 81 | Brain nociceptive imaging in rats using 18f-fluorodeoxyglucose small-animal positron emission tomography. Neuroscience, 2008, 155, 1221-1226. | 1.1 | 32 |
| 82 | ANTINOCICEPTIVE EFFECT OF MORPHINE IN $\hat{I}\pm$ -CHLORALOSE AND ISOFLURANE ANESTHETIZED RATS USING BOLD fMRI. Biomedical Engineering - Applications, Basis and Communications, 2008, 20, 39-46. | 0.3 | 1 |
| 83 | HOW TO EXTRACT THE SPATIAL CORRELATION OF AUDITORY CORTICAL EVOKED POTENTIALS ON MULTIPLE SCALP ELECTRODES IN TINNITUS PATIENTS. Biomedical Engineering - Applications, Basis and Communications, 2008, 20, 297-302. | 0.3 | 0 |
| 84 | DYNAMIC MAPPING OF AMPHETAMINE RESPONSE IN THE RAT BRAIN USING BOLD AND IRON TECHNIQUES. Biomedical Engineering - Applications, Basis and Communications, 2007, 19, 157-163. | 0.3 | 1 |
| 85 | ISPMER: Integrated system for combined PET, MRI, and electrophysiological recording in somatosensory studies in rats. Nuclear Instruments and Methods in Physics Research, Section A: Accelerators, Spectrometers, Detectors and Associated Equipment, 2007, 580, 938-943. | 0.7 | 12 |
| 86 | Exploring nociceptive response by BOLD fMRI in $\hat{l}\pm$ -chloralose anesthetized rats. , 2006, 2006, 33-6. | | 2 |
| 87 | Development of wavelet de-noising technique for PET images. Computerized Medical Imaging and Graphics, 2005, 29, 297-304. | 3.5 | 41 |
| 88 | Spectral Fiber-Photometry Derives Hemoglobin-Absorption Changes for Accurate Measurement of Fluorescent Sensor Activity. SSRN Electronic Journal, 0, , . | 0.4 | 0 |